Flow Enhancement and Cavitation Suppression in Nozzle Flow by Viscoelastic Additives

[1]Homa Naseri*, [1]Phoevos Koukouvinis, [1]Ioannis Karathanassis and [1]Manolis Gavaises

[1]City, University of London, Northampton Square, UK, EC1V 0HB

Abstract

Numerical simulations of turbulent cavitating nozzle flow of Phan-Thien-Tanner and Newtonian fluids are compared to study the effect of viscoelastic additives on cavitation dynamics. The results show that viscoelasticity can stabilize the flow-field and reduce turbulence and vorticity inside the nozzle. Subsequently small scale vortices are suppressed and larger eddies become dominant in the flowfield. Vapor formation in the core of Kelvin-Helmholtz vortices in the shear layer is delayed and overall vapor volume fraction inside the nozzle is reduced by viscoelasticity. Therefore, the density of the two-phase flow passing through the nozzle is higher and the pressure drop across the nozzle is reduced. Hence flow resistance due to turbulence and cavitation inside the nozzle is reduced and the mass flow rate is enhanced.

Keywords: viscoelastic additive; cavitation; turbulence

Introduction

Viscoelastic additives are used in pipelines or district heating/cooling systems as they can contribute to reduction of turbulent drag and cut the pumping costs, however studies about their effect on cavitation in turbulent flows are scarce in the literature. The volumetric efficiency of fuel injection systems can be improved [1] by adding viscoelastic compositions [2] of deposit control additives to fuel blends. Recent experimental evidence [3] suggest that this is due to reduction of cavitation and turbulence in the flow-field by the additive. In this study we examine numerically the effect of viscoelasticity on turbulent cavitating flows similar to the fuel flow in an injector nozzle, in an attempt to provide an explanation for the observed trends.

Viscoelastic fluids are non-Newtonian materials which can exhibit both viscous and elastic properties. They are important for a wide range of applications such as polymer and plastic industries, soft solids, tissue engineering and biological flows. Presence of microstructures such as polymers, surfactants or other particle aggregates in a liquid can often induce viscoelastic properties in fluids which can significantly change the flow behavior even in very low concentrations.

In turbulent flow conditions, polymers can stretch and absorb elastic energy from the near wall eddies, and if they release this energy beyond the buffer layer region in the streamwise direction, they can reduce the turbulence drag and increase the buffer layer thickness [4]. The extensional viscosity of polymeric solutions also inhibits the formation of vortex cavitation in propellers [5]. Moreover, viscoelasticity can alter the dynamics of collapsing bubbles, mainly near solid surfaces [6]. The re-entrant jet motion is retarded and the velocity of the jet formed by bubble collapse is reduced. Therefore the maximum pressure inside the bubble at the final stage of collapse is reduced, which means cavitation damage can be inhibited. However there is a gap in the literature regarding the effect of viscoelasticity on cavitation in turbulent flows and numerical studies can help to establish a better understanding of this effect.

Governing Equations and Simulation Setup

The test case is a step nozzle [7] with cavitation forming at the shear layer of the separated flow as water enters the nozzle with inlet pressure of 2.4 bar into atmospheric pressure and the test rig operates on a steady state condition (see Figure 1). Flow Reynolds number is 27700 based on the mean liquid velocity in the nozzle and nozzle width. Cavitation number is 1.19, defined in the experimental study as:

*Corresponding Author, Homa Naseri: homa.naseri.2@city.ac.uk

$$\sigma = \frac{p_a - p_v}{0.5\rho U^2} \quad (I)$$

where p_a is the atmospheric pressure, p_v is the vapour pressure, ρ is the liquid density and U is the mean velocity of the liquid in the nozzle. This condition corresponds to incipient cavitation regime, therefore it is possible to track the formation, development and collapse of the cavitation structures which all happen inside the nozzle.

	Newtonian	Viscoelastic
Inlet pressure (Pa)	2380000	2380000
Outlet pressure (Pa)	101325	101325
Vapour pressure (Pa)	2340	2340
Viscosity (Pa.s)	0.00102	0.00102
Polymer Viscosity(Pa.s)	-	0.009
Relaxation time (s)	-	0.04

Table 1. Fluid properties and boundary conditions for the simulations

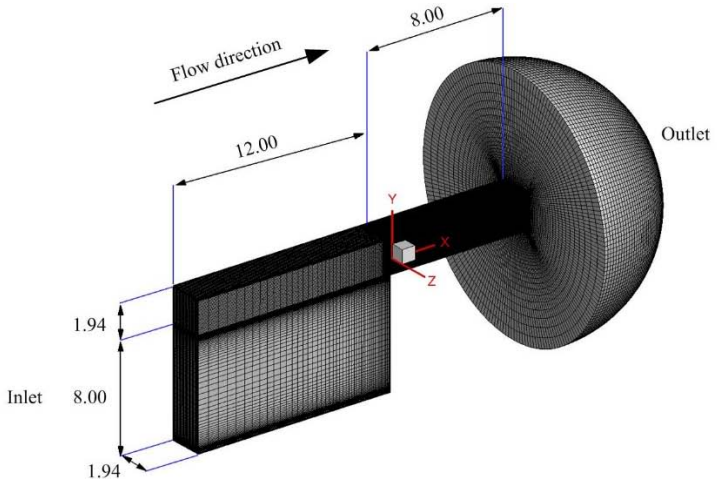

Figure 1. Simulations conditions, computational domain and geometry dimensions (in mm)

Description and details of the numerical framework employed for the Newtonian flow simulation as well as the experimental procedures can be found in [7] and [8]., therefore only a brief description of the simulation setup details are presented here. This problem concerns a two phase flow and the mixture model is used to describe the fluid. In mixture framework, the continuity and momentum equations are solved for a mixture of liquid and vapor phase, then pressure data is used by the cavitation model to obtain the volume fraction of each phase. The continuity and momentum equations are:

$$\frac{\partial \rho_m}{\partial t} + \nabla.(\rho_m \boldsymbol{u}) = 0 \quad (II)$$

$$\frac{\partial \rho_m \boldsymbol{u}}{\partial t} + \nabla.(\rho_m \boldsymbol{u} \otimes \boldsymbol{u}) = -\nabla p + \nabla.\boldsymbol{\tau} + \nabla.\boldsymbol{\tau_v} \quad (III)$$

where ρ_m is the mixture density, $\boldsymbol{\tau}$ is the stress tensor and $\boldsymbol{\tau_v}$ is the viscoelastic stress tensor.

The constitutive equation for the viscoelastic fluid is based on the linear Phan-Thien-Tanner model [9], this model assumes polymers form entangled networks where the junctions can be destroyed and re-created:

$$\lambda \overset{\nabla}{\boldsymbol{\tau}}_v + f(\mathrm{tr}(\boldsymbol{\tau}_v)).\boldsymbol{\tau} = \mu_p(\nabla \boldsymbol{u} + \nabla \boldsymbol{u}^T) \quad (IV)$$

where μ_p is the polymer viscosity and f(tr($\boldsymbol{\tau}_v$)) is defined as:

$$f(\mathrm{tr}(\boldsymbol{\tau}_v)) = 1 + \varepsilon \frac{\lambda}{\mu_p}(\mathrm{tr}(\boldsymbol{\tau}_v)) \quad (V)$$

where λ is the polymer relaxation time, ε is taken 0.02 for dilute solutions and $\overset{\nabla}{\boldsymbol{\tau}}_v$ is the Oldroyd upper convective derivative, defined as:

$$\overset{\nabla}{\boldsymbol{\tau}}_{\mathrm{v}} = \frac{D\boldsymbol{\tau}_{\mathrm{v}}}{Dt} - (\nabla \boldsymbol{u}.\boldsymbol{\tau}_{\mathrm{v}} + \boldsymbol{\tau}_{\mathrm{v}}.\nabla \boldsymbol{u}^{\mathrm{T}}) \qquad (VI)$$

The polymer relaxation time is taken from properties of dilute solutions of polyisobutylene in tetradecane [10]. An artificial diffusion term is added to the viscoelastic constitutive equation for numerical stability, such that the dimensionless artificial diffusivity ($D = k/u_\tau H$, where k is the constant artificial diffusivity, u_τ is the friction velocity and H is the nozzle width) remains below 0.01.

To model cavitation, the mass transfer rate model of Schnerr and Sauer [11] is used, and turbulence is modelled using the WALE LES formulation [12]. Inside the nozzle the grid spacing is 20 µm which is below the Taylor length scale of the in-nozzle flow and near the wall the resolution is 2.5 µm giving y^+ values of 0.5. The time step is 1µs for CFL number of 0.5 and for the viscoelastic case the time step is reduced to 0.5 µs for a CFL number of 0.25. Inlet and outlet pressures and no-slip wall boundary conditions are used. Grid dependency and performance of turbulence and cavitation models was previously validated against LDV measurements of velocity and RMS of turbulence velocity [8]. The fluid properties and boundary conditions used for the simulations are summarized in table 1.

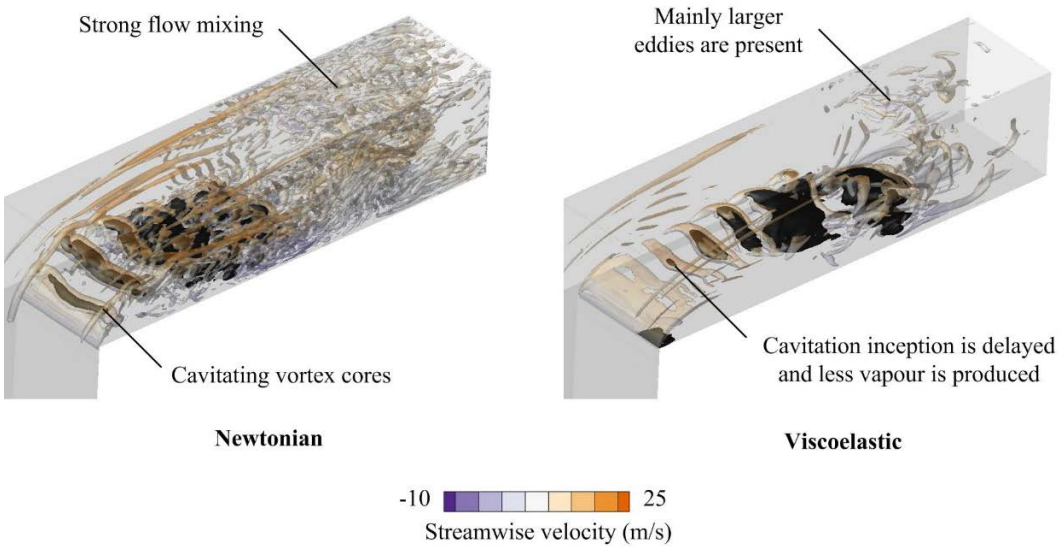

Figure 2. Isosurfaces of second invariant of velocity gradient at 1E+9 s^{-2} colored with streamwise velocity and isosufaces of 50% vapor volume fraction (black color)

The flow topology in terms of the second invariant of the velocity gradient is displayed in Figure 2 for the Newtonian and the viscoelastic fluid. It is evident that turbulent flow structures present in the Newtonian fluid are strongly suppressed by viscoelasticity. Moreover, formation of K-H vortices and development of cavitation vapor in their core is delayed in the viscoelastic fluid. Furthermore, the size of the cavitation cloud is smaller in the viscoelastic fluid. After the breakdown of the vortex sheet, a strong flow mixing happens in the Newtonian fluid, whereas the mixing is strongly suppressed in the viscoelastic fluid. Moreover, small-scale vortices are inhibited by viscoelasticity and only larger eddies last.

In Figure 3 cavitation structures in the Newtonian and the viscoelastic fluid are presented in terms of the isosurface of 50% vapor volume fraction. It is evident that the shape of the cavitation clouds is different in the two fluids; the vapor structures appear smoother in the viscoelastic fluid and the size of the vapor cloud is smaller. The more homogeneous cavitation isosurface in the viscoelastic fluid can be due to the reduced level of flow perturbations and damping of small scale turbulence in this fluid as demonstrated in Figure 2.

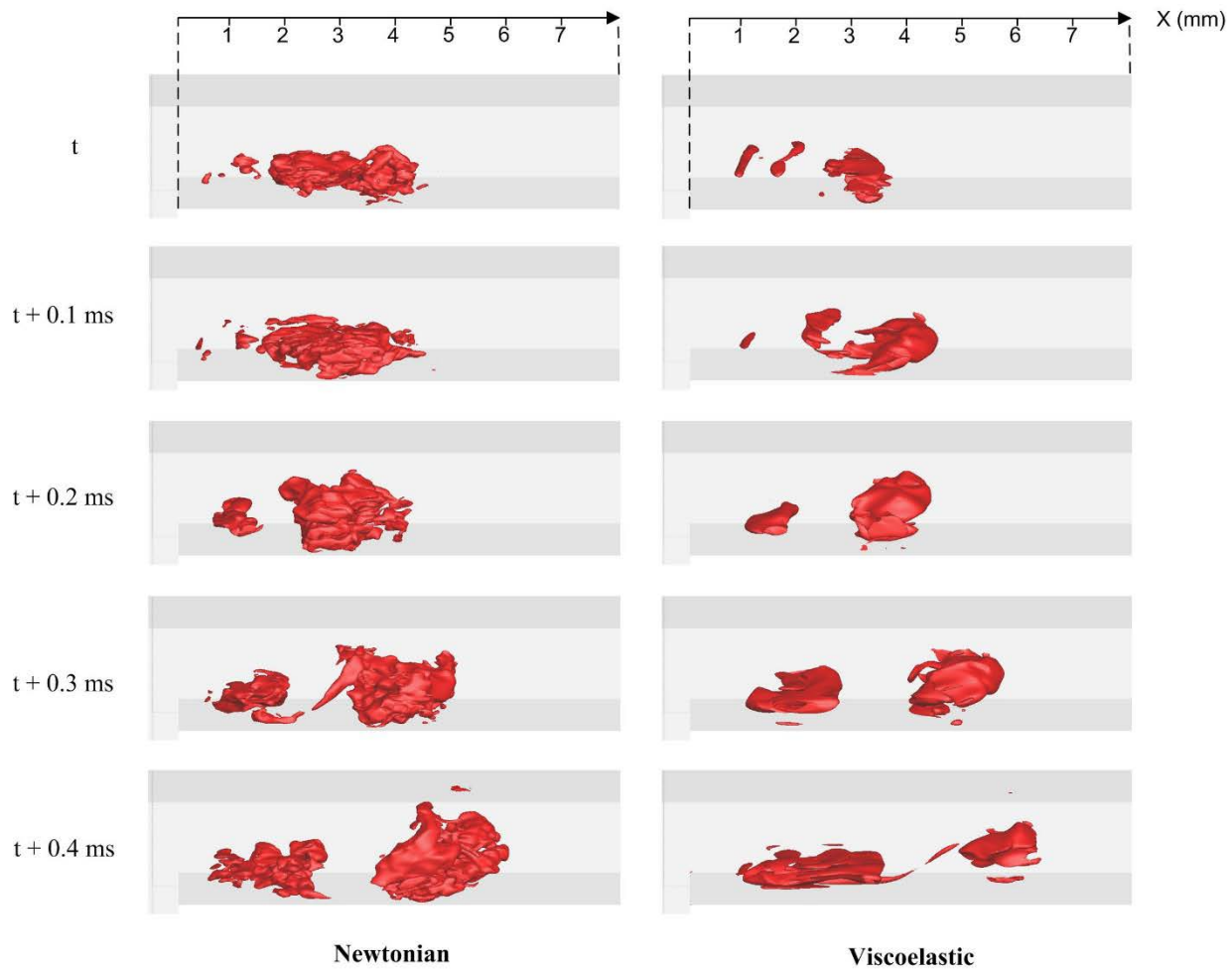

Figure 3. Evolution of the cavitation cloud topology in the Newtonian and the viscoelastic fluid, Isosurfaces represent the regions of 50% vapor volume fraction

Additionally, fluctuations of the mass flow rate at the exit of the nozzle is measured and the dominant frequencies of fluctuations are identified using FFT. For the viscoelastic fluid, a dominant frequency of 57 Hz is identified, whereas in the Newtonian fluid the frequency is increased to 168 Hz. Reduction of the frequency of mass flow rate fluctuations in the viscoelastic fluid indicates that the shedding of the cavitation cloud is also less frequent. Moreover, wall-normal velocity fluctuations are reduced along the nozzle length by ~30%, which directly shows the turbulence suppression property of the viscoelastic additive.

The time variation of the fluid density inside the nozzle is plotted in Figure 4 (a) presenting three cycles of cavitation formation and shedding. The fluid density in the Newtonian case is constantly below the viscoelastic fluid density, indicating a higher liquid fraction and hence cavitation suppression in the viscoelastic fluid. In Figure 2 it was demonstrated that the turbulent eddies observed in the Newtonian fluid are partly suppressed in the viscoelastic fluid, therefore it is expected that vorticity levels would also be lower in the viscoelastic fluid. This data is presented in Figure 4 (b) which shows the magnitude of the streamwise vorticity inside the nozzle for the two fluids. Vorticity magnitude in the Newtonian fluid is higher in all locations inside the nozzle as it can also be seen in the contour plots (Figure 4 (c)), in fact streamwise vorticity magnitude is reduced by ~88% inside the whole nozzle for the viscoelastic fluid. Moreover, regions of peak vorticity corresponding to the vortex cores in Figure 4 (c), are in agreement with observations of Figure 2 showing that smaller eddies are suppressed by viscoelasticity and large scale vortices become more dominant. It is also noted that vorticity generation downstream of the recirculation region (x>4 mm) is strongly suppressed in the viscoelastic fluid.

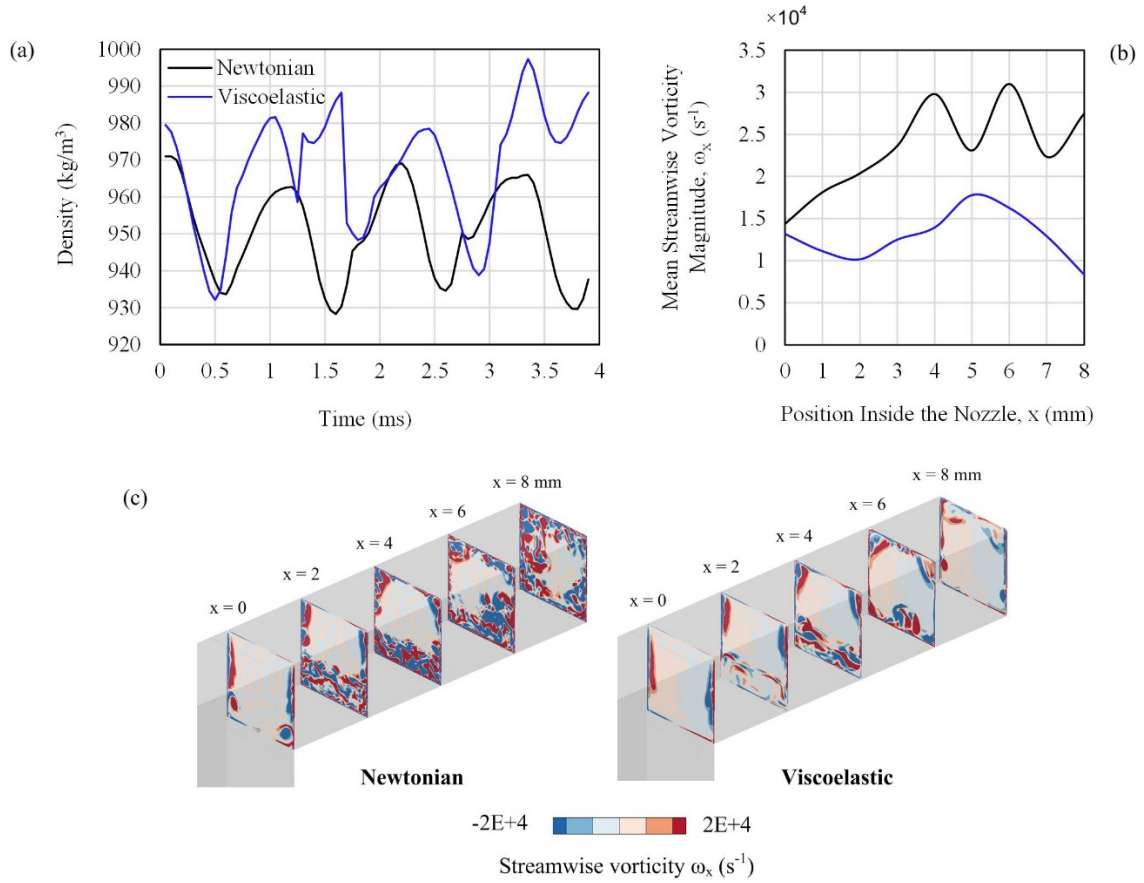

Figure 4. (a) Density variations inside the nozzle during three cavitation cycles, (b) magnitude of the streamwise vorticity, mean value is calculated in planes along the nozzle length, (c) contour plots of streamwise vorticity inside the nozzle

The time averaged pressure and vapor volume fraction data inside the nozzle are presented in Figure 5. Pressure in the cavitation cloud region (~1 mm<x<~5 mm) is increased in the viscoelastic fluid on average by ~3.5 KPa. Furthermore the pressure drop across the nozzle is also reduced in the viscoelastic fluid, which can be because of the reduction of form drag due to smaller size of the cavitation and recirculation region and also less turbulent drag. The reduction of vapor volume fraction in the viscoelastic fluid is more pronounced, where the cavitation volume fraction inside the nozzle is decreased by ~40%, indicating that more liquid is being delivered in the viscoelastic flow. Suppression of cavitation and reduction of turbulence level in the nozzle result in flow enhancement and so the mass flow rate is increased by ~2.2% through the nozzle in the viscoelastic fluid.

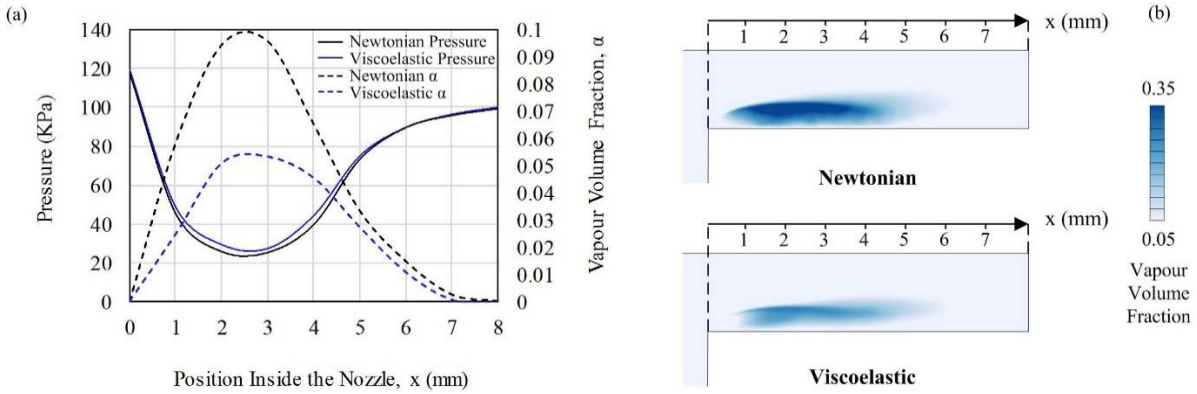

Figure 5. (a) Time-averaged data for pressure and vapor volume fraction inside the nozzle, (b) contour plots of time-averaged vapor volume fraction in the midplane of the nozzle

Conclusion

In this study we compared cavitation formation and development inside a nozzle for Newtonian and Phan-Thien-Tanner viscoelastic fluids. Turbulent flow structures visualized by the second invariant of the velocity gradient are strongly suppressed in the viscoelastic fluid. Development of vapor in the core of the shear layer K-H vortices is delayed and a smaller cavitation cloud is formed. Small scale vortices are damped and larger vortices become dominant in the flow, while streamwise vorticity is reduced. Time-averaged statistics show that vapor volume fraction is smaller in the viscoelastic fluid, hence the density of the fluid passing through the nozzle is increased.
Overall, pressure losses across the nozzle by turbulence drag and form drag due to cavitation and flow recirculation are suppressed in the viscoelastic fluid, resulting in an improved flow rate.

References

[1] R. H. Barbour, R. Quigley, and A. Panesar, “Investigations into Fuel Additive Induced Power Gain in the CEC F-98-08 DW10B Injector Fouling Engine Test,” 2014.
[2] R. H. Barbour, “Method to provide power gain in an engine,” 2011.
[3] H. Naseri, K. Trickett, N. Mitroglou, I. Karathanassis, P. Koukouvinis, M. Gavaises, R. Barbour, D. Diamond, S. E. Rogers, M. Santini, and J. Wang, “Turbulence and Cavitation Suppression by Quaternary Ammonium Salt Additives,” 2018.
[4] Y. Dubief, C. M. White, V. E. Terrapon, E. S. Shaqfeh, P. Moin, and S. K. Lele, “On the coherent drag-reducing and turbulence-enhancing behaviour of polymers in wall flows,” *J. Fluid Mech.*, vol. 514, pp. 271–280, 2004.
[5] C. T. Hsiao, Q. Zhang, X. Wu, and G. L. Chahine, “Effects of Polymer Injection on Vortex Cavitation Inception,” in *28th Symposium on Naval Hydrodynamics*, 2010.
[6] E. A. Brujan, T. Ikeda, and Y. Matsumoto, “Dynamics of ultrasound - induced cavitation bubbles in non - Newtonian liquids and near a rigid boundary,” *Phys. Fluids*, vol. 16, no. 7, pp. 2402–2410, 2004.
[7] A. Sou, B. Biçer, and A. Tomiyama, “Numerical simulation of incipient cavitation flow in a nozzle of fuel injector,” *Comput. Fluids*, vol. 103, pp. 42–48, 2014.
[8] Koukouvinis, H. Naseri, and M. Gavaises, “Performance of turbulence and cavitation models in prediction of incipient and developed cavitation,” *Int. J. Engine Res.*, vol. 18, no. 4, pp. 333–350, 2016.
[9] N. P. Thien and R. I. Tanner, “A new constitutive equation derived from network theory,” *J. Nonnewton. Fluid Mech.*, vol. 2, no. 4, pp. 353–365, 1977.
[10] D. N. Sibley, “Viscoelastic Flows of PTT Fluids,” University of Bath, 2010.
[11] G. H. Schneer and J. Sauer, “Physical and Numerical modelling of unsteady cavitation dynamics,” *Int. Conf. Multiph. Flow*, vol. 11, no. 4, pp. 391–400, 2001.
[12] F. Nicoud and F. Ducros, “Subgrid-scale stress modelling based on the square of the velocity gradient tensor,” *Flow, Turbul. Combust.*, vol. 62, no. 3, pp. 183–200, 1999.